

## Performance of a seawater desalination system coupled with a nuclear heating reactor under off-design operating conditions

Xiaoze Du<sup>a\*</sup>, Shaorong Wu<sup>b</sup>, Lijun Yang<sup>a</sup>

<sup>a</sup>*Department of Power Engineering, North China Electric Power University (Beijing), Beijing 102206, China  
Tel. +86 (10) 8079-8627; Fax +86 (10) 8079-8618; email: duxz@ncepubj.edu.cn*

<sup>b</sup>*Institute of Nuclear Energy Technology, Tsinghua University, Beijing 100084, China*

Received 16 August 2004; accepted 7 October 2004

---

### Abstract

In order to understand the performance of a large-capacity VTE–MED nuclear seawater desalination system thoroughly, the responding characteristics of the system to the off-design operating conditions were studied. The influence of scale deposit in tubes on the heat transfer areas needed and on the heat transfer coefficients with high top boiling temperature (TBT) was illustrated. The decrease of GOR, and also the damage to the normal operation of the system caused by temperature drop of feed brine because of seasonal variation, were explored, based on which a corresponding approach for adjusting feed brine flow rate was proposed. An optimal brine feed flow rate was also proposed to obtain the highest GOR under different heat loadings. The work could be helpful for the efficient and safe operation of nuclear VTE–MED desalination plants.

**Keywords:** Seawater desalination; Nuclear heating reactor; Multi-effect distillation

---

### 1. Introduction

The multi-effect distillation (MED) process with a vertical tube evaporator (VTE) is generally accepted to be one of the most efficient desalination technologies. Having overcome the impediments of scaling and corrosion in the system successfully with the technological developments in materials and techniques, the market share of VTE–MED systems has been increasing steadily

over the past decades [1]. Besides, the long-term stability of nuclear fuel prices and the low level of CO<sub>2</sub> and NO<sub>x</sub> emissions warrant special attention to using nuclear energy for seawater desalination [2–4]. As the international highlight to extend the application of nuclear energy for seawater desalination recommended by the IAEA, the VTE–MED system coupled with a low-temperature nuclear heating reactor (NHR) has proved to be a promising alternative for the solution of potable water shortages [4,5].

---

\*Corresponding author.

In our previous studies we established the physical and mathematical model for a large-capacity VTE–MED system coupled with NHR and discussed its thermal hydraulic performance under the designed operating conditions [5]. Also we have taken a preliminary optimization analysis on the design parameters of the system [6]. However, for an accomplished seawater desalination system, most of its operating parameters are not on the designed values, of which the most important ones may include the variations of the feed brine temperature due to the season's alternation, the effect of scaling on the decrease of heat transfer coefficients of the system, and also, the characteristics of the desalination system to the load variation of the coupled NHR. Therefore, it is necessary to investigate the dynamic characteristics of the system under unsteady operating conditions in order to understand the performance thoroughly of a designed VTE–MED system.

Several researchers have investigated the dynamic performances of the multi-effect distillation system by theoretical modeling or experimental studies, including that of the start-up, load variation and troubleshooting of the system [7–9]. In order to simplify the control equations, most dynamic models take one effect as a node of the system without considering the variations of the thermal hydraulic characteristics in the effect. Most recently, Shivayyanamath and Tewari [10] simulated the start-up characteristics of a multi-stage flash desalination plant considering the variations of thermodynamic properties with temperature and salinity stage by stage. However, few studies focus on system performances with variation of the operating conditions. In the present paper, such works are taken based on the non-linear mathematical models developed [5] by considering the evolution of the thermal hydraulic performance in the effect during the evaporation of brine.

## 2. Summary of a nuclear VTE–MED seawater desalination system [5]

The VTE–MED seawater desalination system takes the saturated steam at 123°C provided by the NHR as the source vapor. The system includes 28 effects, each of which includes one evaporator and one pre-heater with a tube-in shell arrangement. The output vapor of the last effect flows to the bottom condenser where the feed brine is preheated. The system is designed with a temperature distribution scheme of an in-section equal heat transfer area. Except to the first effect evaporator, the areas of evaporators and pre-heaters of every seven effects are equal. The schematic illustration of the physical model is shown in Fig. 1. The detail describes the system, and the steady thermal hydraulic performances can be referred to from the literature [5]. On the designed operating conditions, the feed brine rate is about two times that of the fresh output water. The average temperature of the input feed brine is designed at 25°C, based on which the inlet feed brine temperature of the last effect pre-heater can be heated to 35°C by the bottom condenser. Then the feed brine flows through the total 28 pre-heaters in turn. Under the standard operating conditions, the inlet feed brine temperature of the first effect evaporator can reach 120°C.

The heat transfer at every evaporator includes that of the condensation of the source vapor on the outside wall and the evaporation of the vertical falling liquid film on the inside wall. The overall heat transfer coefficient of the evaporator,  $K$ , can be obtained by:

$$\frac{1}{K} = \frac{r_B - \delta_S}{r_V \alpha_V} + \frac{r_B - \delta_S}{k_W / \log(r_V / r_B)} + \frac{r_B - \delta_B}{k_S / \log[r_B / (r_B - \delta_S)]} + \frac{1}{\alpha_B} \quad (1)$$

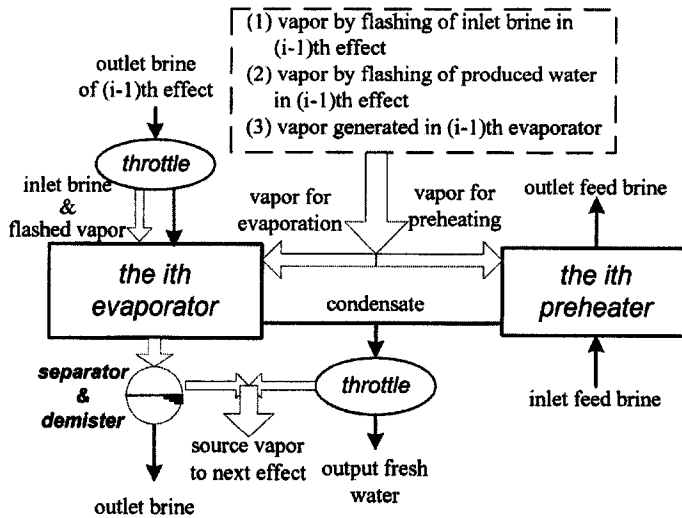


Fig. 1. Schematic diagram of physical model.

Considering the boiling point elevation (BPE) of the brine with salinity due to evaporation, and neglecting the heat loss, the local heat transfer equation in the evaporator can be expressed as:

$$-\left[\gamma_B + c_p (T_{B,z} - T_B)\right] \frac{dW_B}{dz} = \gamma_V \frac{r_V}{r_B - \delta_S} \frac{dW_V}{dz} \quad (2)$$

$$= K (T_V - T_{V,z})$$

The discretization of the governing equation is taken along the tube length, and the variation of the brine flow rate in the effect can be then acquired numerically. During the solution, the thermal properties of the brine are thought to be constant at every integral grid. However, the saturation temperature and other thermal properties will be updated before solving the equations at the next grid according to the newly obtained salinity of brine due to evaporation. The influences of the BPE on distillation can be then considered in the model.

Each pre-heater is a countercurrent tube-in-shell condenser. The performance parameters can be obtained by the method of the logarithmic mean temperature difference.

The enthalpy of brine or fresh water will remain constant after throttling. Taking  $x$  as the expression of the flashing ratio, based on energy conservation, we have

$$x = \frac{h'_1 - h'_2}{h''_2 - h'_2}$$

where subscripts 1 and 2 refer to the thermodynamic states before and after throttling, respectively, and  $h''$  and  $h'$  are the enthalpy of saturated vapor and saturated liquid, respectively. The flashing vapor of brine is added to the vapor generated in the next effect, while that of fresh water is added to the vapor outcome of the present effect.

### 3. Influence of scale deposit on the brine side

Scaling is one of the main restrictions to the application of the VTE–MED technique in seawater desalination, especially for high-temperature processes. While increasing the top boiling temperature (TBT), the system can include more effects to obtain greater GOR. However, the

scaling of calcium carbonate on the brine side will impede the improvement of system performance obviously if the TBT is 75°C or higher. Moreover, the scaling of calcium sulphate on the brine side will have an obvious influence on the system performance if TBT is about 120°C. For the present high-temperature VTE–MED system, it is necessary to analyze the influences of scaling on the brine side.

Numerous researchers have been devoted to studies of scale inhibitors and anti-scalants [11–13]. According to our experimental data, and also the related reports in the literature, it is assumed that the scaling thickness in the brine side,  $\delta_s$ , would not be greater than 10  $\mu\text{m}$  in 3 years after the start-up of the system. From then on the thickness of the scale would be constant by the programming pretreatment of feed brine and other periodic anti-scaling techniques. For this reason, the paper focuses on the system performance variations with the scale thickness from 0 to 10  $\mu\text{m}$ . The design parameters of the system were selected to ensure that the coupled heat resource from NHR can reach 200 MW when the scaling thickness is as high as 10  $\mu\text{m}$ ; therefore, the variation of scale thickness has no obvious effect on the fresh water output and GOR in the first 3 years after start-up of the system. Fig. 2 compares the average heat transfer coefficients of clean tubes to that of the tubes with the scaling thickness of 10  $\mu\text{m}$  at each effect. It is seen that the scaling on the brine side in the tubes can obviously lead to a decrease of heat transfer coefficients either in the evaporator or in the pre-heater; consequently, the heat transfer areas of each effect needed to increase. Fig. 3 shows the variation of the utilization ratio of the total heat transfer areas of the system with scaling thickness. Only about 65% of the designed heat transfer areas of the system are needed to consume the source heat rate of 200 MW from the NHR and to reach the designed GOR without considering the influence of scaling.

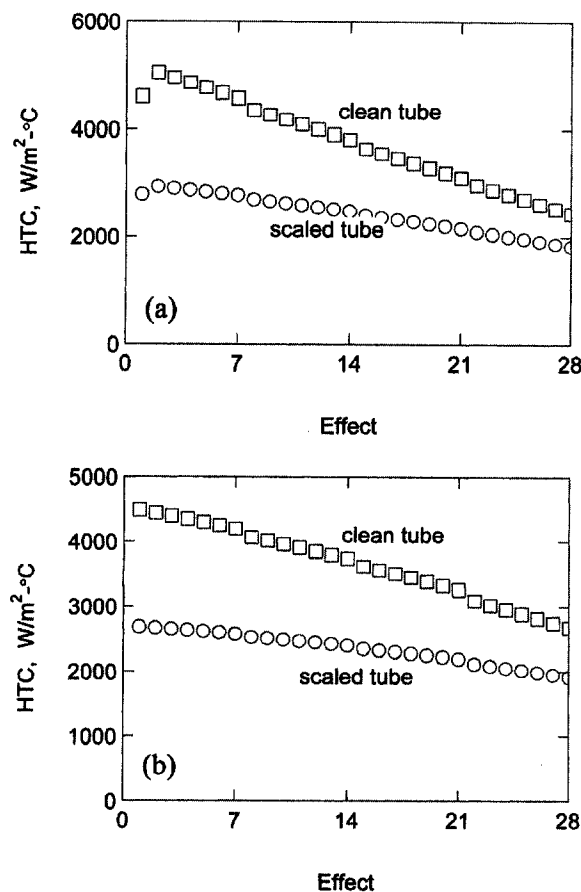


Fig. 2. Influence of deposit of scale on the average heat transfer coefficients (HTC) of each effect. (a) Evaporator; (b) Preheater.

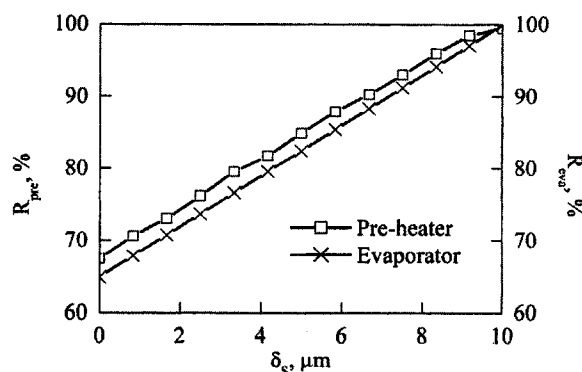


Fig. 3. Ratio of utilization of heat transfer areas of the system with scaling thickness.

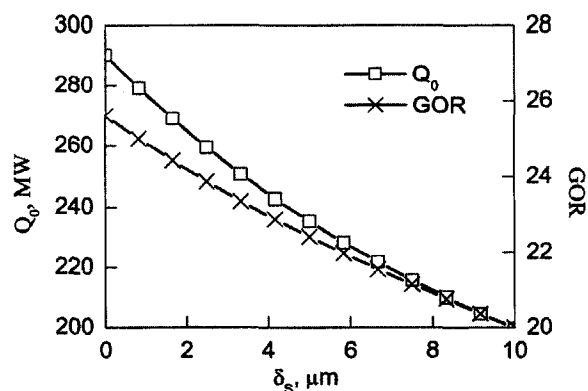


Fig. 4. Effect of scaling thickness on source heat flow rate and GOR.

For different scaling thickness of 0 to 10  $\mu\text{m}$ , the latent ability of the system to consume the source heat rate and also the corresponding GOR are illustrated in Fig. 4. With decreasing scaling thickness, the source heat rate in the first effect can reach as high as 290 MW, which is far greater than the designed value of 200 MW, while GOR of the system can reach 25.7.

#### 4. Responding performance of the system with variation of operating parameters

##### 4.1. Effect of seasonal drop of feed brine temperature on system performance

The present system was designed so that the pretreated feed brine was preheated in the bottom condenser by the saturated vapor generated from the last effect, and then entered the last effect preheater. The designed temperature of the feed brine,  $T_{\text{sea,in}}$ , is 25°C, which can be heated to 35°C in the bottom condenser at the designed conditions. However, the feed brine temperature may have a departure from the designed value due to seasonal alternation. Under the conditions that the feed brine temperature is higher than 25°C, the outlet feed brine temperature of the bottom condenser can be controlled to be 35°C by increasing

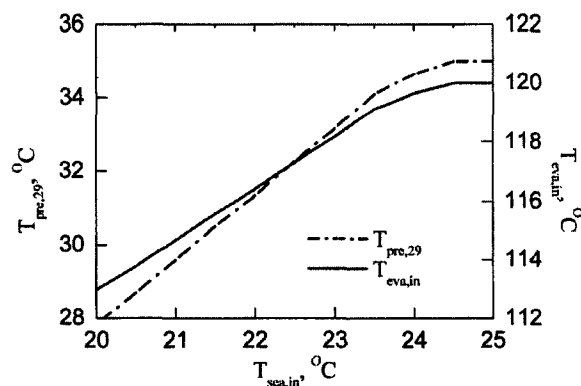


Fig. 5. Influence of the variation of feed brine temperature,  $T_{\text{sea,in}}$  on the outlet brine temperature of last effect condenser and on the inlet brine temperature of first effect evaporator

the feed brine rate. On the contrary, if the feed brine temperature is lower than the designed value, 25°C, the outlet feed brine temperature of the bottom condenser cannot reach the designed value. Fig. 5 shows such results by illustrating the relationships of the inlet feed brine temperature,  $T_{\text{sea,in}}$ , with the inlet brine temperatures of the last effect preheater,  $T_{\text{pre,29}}$ , and the first effect evaporator,  $T_{\text{eva,in}}$ , respectively, from which one can find that the inlet brine temperature of the first effect evaporator also decreases, leading to brine sub-cooling.

In order to reach the designed TBT, part of the source heat has to be consumed to preheat the brine in the evaporator; as a result, the source vapor used to evaporate the brine will decrease in the first effect. As shown in Fig. 6, this leads to the reduction of the fresh water output of all effects, and consequent decrease in GOR of the system even though the first effect evaporator has enough heat transfer area. In fact, because of the relatively low heat transfer coefficient of the single-phase flow in the inlet part of the first effect evaporator to preheat the brine, the heat transfer area needed in the first effect evaporator also increases with decreasing feed brine temperature. Then the area of brine evaporation will

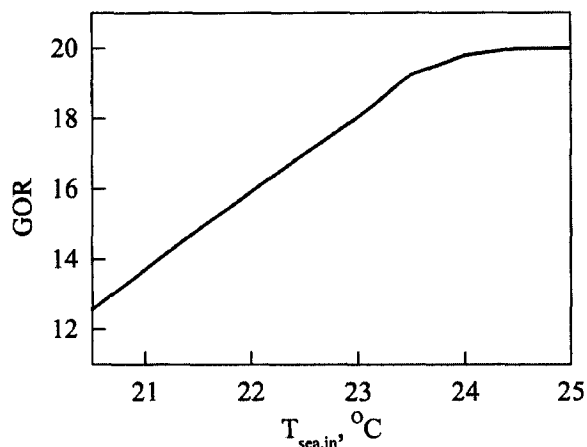


Fig. 6. Influences of the variation of feed brine temperature,  $T_{sea,in}$ , on GOR of the system.

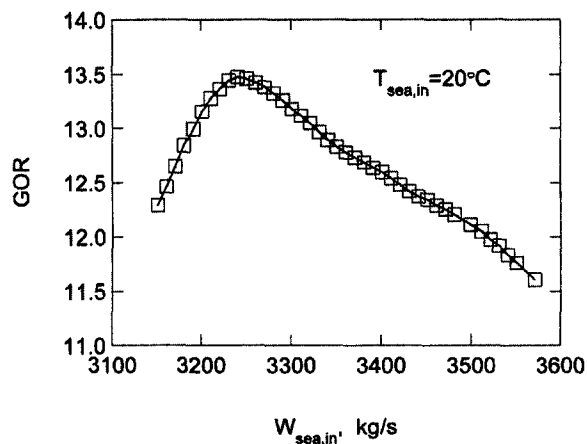


Fig. 8. Influences of the feed brine flow rate on GOR while the inlet feed brine temperature,  $T_{sea,in}$ , is 20°C.

also decrease. Fig. 7 shows the influences of inlet feed brine temperature on the ratio of the heat transfer area and source vapor to preheat brine in the first effect evaporator. This indicates that all of the first effect area will be used to preheat the brine as the inlet feed brine temperature is lower than about 21.8°C, which means that no vapor can be generated in the first effect to provide the source heat for the following effects, and there is no fresh water output in the system.

Therefore, the feed brine flow rate has to be varied with the decrease of the inlet temperature

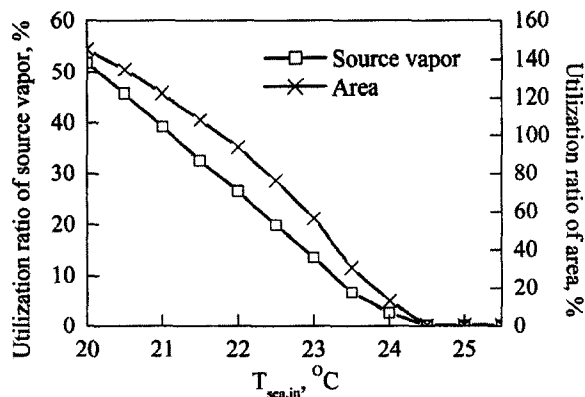


Fig. 7. Influences of inlet feed brine temperature,  $T_{sea,in}$ , on the ratio of heat transfer area and source vapor to preheat brine in the first effect evaporator.

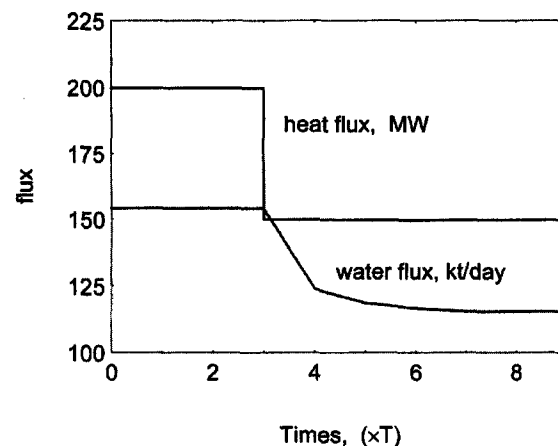


Fig. 9. Variation of fresh water product with time (expressed by operating cycle time,  $T$ ) while the heating power of NHR is steeply reduced.

in order to eliminate the sub-cooling of the inlet brine in the first effect evaporator. We find that there is an optimal flow rate of the feed brine at every inlet temperature, which can ensure that minimum source heat is consumed to preheat the brine in the first effect evaporator, and as a result, the largest GOR is acquired under the conditions. Fig. 8 illustrates the influences of the feed brine flow rate on GOR while the inlet feed brine temperature is 20°C. The optimal flow rate of the feed brine is about 3240 kg/s, of which the inlet

temperature of brine in the first evaporator can reach the designed value, 120°C, and the GOR of the system is 13.5.

#### 4.2. Response of fresh water output to the step reduction of source vapor flow

Another important operating parameter to affect the performance of the seawater desalination system is the source vapor flow rate from the NHR. If there are any variations of the source vapor output from the NHR, the fresh water output of the system will also vary. Fig. 9 shows the variation of fresh water product with time (operating cycle) while the heating power of NHR is reduced steeply to 150 MW from 200 MW. The corresponding variations of inlet brine temperature of the first effect evaporator are shown in Fig. 10. The reduction of the source heating power leads to the decrease of the source vapor used to evaporate the brine in the first effect. As a result, the vapor generated in the following effects will also decrease in turn. While the variation affects the last effect at the end of the current operating cycle, the reduction of vapor generated results in a decrease of the outlet feed brine temperature of the bottom condenser. As in the previous analysis, the inlet brine temperature of the first effect evaporator is then subcooled to consume more source heat for preheating. The vapor generated in the first effect will decrease more. As shown in Fig. 9, the system will operate in a low fresh water output steadily after several operating cycles.

#### 4.3. Influence of step reduction of feed brine on system performance

The direct influence of step reduction of the feed brine flow rate is the variation of the system loading; in other words, there is not a great enough cooling source to condense the vapor generated. Firstly, the resulting reduction of the apparent heat to preheat the feed brine means that

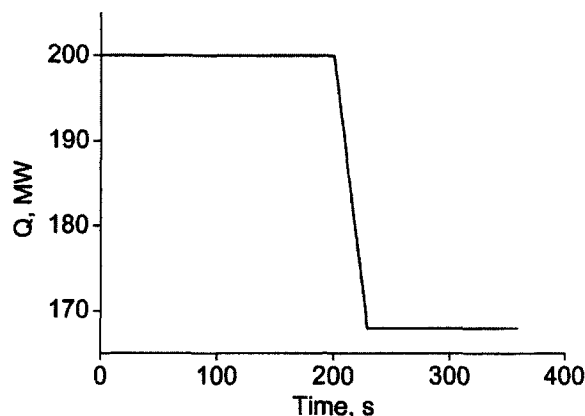


Fig. 10. Variation of heat loading of the nuclear heating reactor with time while feed brine flow rate is steeply reduced.

the vapor generated from last effect cannot be totally condensed, which results in the reduction of the fresh water output of the system. Secondly, the outlet temperature of the feed brine at the bottom condenser will be higher than the designed value. The overheated feed brine also cannot condense the vapor generated in the former preheaters, which reduces the fresh water output in more effects. If the over-preheated feed brine enters the first effect evaporator, the consumption of the source heat from NHR will be reduced abruptly, which means that the loading of the NHR is consequently reduced.

It is very important to determine the time period between the step reduction of feed brine and the loading reduction of NHR. With the step reduction of the feed brine flow rate, the time-based variations of the loading of NHR are illustrated in Fig. 10. One can find that the heat loading of NHR will be reduced steeply from 200 MW to about 160 MW after about 220 s due to the reduction of the feed brine flow rate.

#### 4.4. Characteristics of the feed brine flow rate to the source vapor loading

There are two contrary influences of the feed brine flow rate on the fresh water output of the

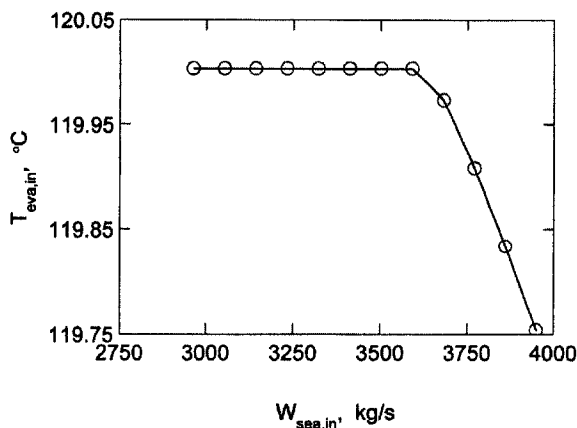


Fig. 11. Influence of feed brine flow rate on the inlet brine temperature of the first effect evaporator.

system. On the one hand, more source vapors are needed to preheat the brine under the higher feed brine flow rate, which leads to a decrease of the heat source used to evaporate the brine in the evaporator. If the feed brine rate is continuously increased, it is possible that the heat transfer rate of preheaters cannot afford to preheat the brine to the designed temperature. As shown in Fig. 11, this will cause the brine to be subcooled in the first effect evaporator and decrease the fresh water output too. On the other hand, a higher feed brine flow rate may increase the heat transfer coefficient in the tube and also increase the flash vapor generated. Obviously this influence of an increasing feed brine flow rate will benefit the fresh water output. For these reasons, there is the optimal feed brine flow rate under a given source of heat power under which the system can have the best fresh water output. Therefore, it is necessary to adjust the feed brine flow rate according to the variations of the source heat loading from the NHR.

Fig. 12 illustrates the variations of fresh water output with feed brine flow rate under different source heat rates of the first effect. The real line in the figure shows the optimal brine flow rate under different source heat power. For example, while the source heat power is 150 MW, it is

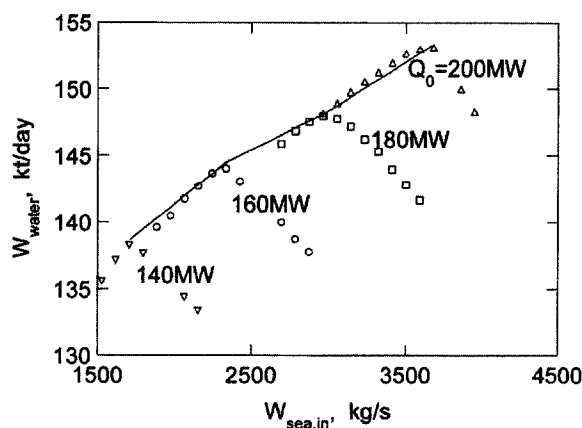


Fig. 12. Variations of fresh water output with feed brine flow rate under different source heat rates of the first effect.

found that the fresh water output of the system can reach 140,000 t/d under the optimal feed brine flow rate, compared with Fig. 9 where the fresh water output is less than 120,000 t/d without adjusting the feed brine flow rate.

## 5. Conclusions

The dynamic responses to the variations of the operating conditions of a designed large-capacity VTE–MED nuclear seawater desalination system were explored based on the developed mathematical model. The influence of scale deposit in the tubes on the heat transfer areas and on the heat transfer coefficients with a high TBT was illustrated. The decrease of GOR, and also the damage to the normal operation of the system caused by temperature drop of feed brine because of seasonal variation, were explored based on which a corresponding approach of adjusting the feed brine flow rate was proposed. The characteristics of the feed brine flow rate to the source vapor loading were also discussed. The results indicate that the feed brine flow rate has two contrary influences on fresh water output of the system. Under different sources of heat flux, the optimal brine feed flow rate to obtain the highest



GOR was discussed. The present work would be helpful for the efficient and safe operation of large-capacity nuclear VTE–MED desalination plants.

$V$  — Vapor  
 $S$  — Scale  
 $W$  — Tube wall

## 6. Symbols

$c_p$  — Specific heat of brine, J/(kg°C)  
 $h$  — Enthalpy, J/kg  
 $K$  — Overall heat transfer coefficient, W/(m<sup>2</sup> °C)  
 $k$  — Conductivity, W/(m°C)  
 $r$  — Radius of tube, m  
 $T$  — Temperature, °C  
 $W$  — Flow rate, kg/s  
 $x$  — Flashing ratio of brine after throttling  
 $z$  — Coordinate down the tube

### Greek

$\alpha$  — Convective heat transfer coefficient, W/(m<sup>2</sup>°C)  
 $\gamma$  — Latent heat, J/kg  
 $\delta_s$  — Thickness of scale, m

### Subscripts

0 — Source  
 $B$  — Brine

## References

- [1] M. Al-Shammiri and M. Safar, Desalination, 126 (1999) 45–59.
- [2] J. Kupitz and T. Konishi, Kerntechnik, 62 (1997) 254–259.
- [3] W. Nooijen and J. Wouters, Desalination, 89 (1992) 1–20.
- [4] P.J. Gowin and T. Konishi, Desalination, 126 (1999) 301–307.
- [5] S. Wu, X. Du and L. Cheng, Desalination, 140 (2001) 297–307.
- [6] S. Wu and X. Du, Desalination, 155 (2003) 171–178.
- [7] H.A. Narmine and M.A. Marwan, Desalination, 114 (1997) 189–196.
- [8] M. Noda, T. Chida, S. Hasebe and I. Hashimoto, Computer Chem. Engn., 24 (2000) 1577–1583.
- [9] M. Darwish, N. Al Najem, T. Froment and J. de Gunzbourg, Desalination, 74 (1989) 277–288.
- [10] S. Shivayyanamath and P.K. Tewari, Desalination, 155 (2003) 277–286.
- [11] R. Semiat, I. Sutzkover and D. Hasson, Desalination, 159 (2003) 11–19.
- [12] I. Atamanenko, A. Kryvoruchko, L. Yurlova and E. Tsapiuk, Desalination, 147 (2002) 257–262.
- [13] J.S. Gill, Desalination, 124 (1999) 43–50.